

# Animal Model

## Mice with Homozygous Disruption of the *mdr2* P-Glycoprotein Gene A Novel Animal Model for Studies of Nonsuppurative Inflammatory Cholangitis and Hepatocarcinogenesis

Thais H. Mauad,\*  
Carin M. J. van Nieuwkerk,\*†  
Koert P. Dingemans,\* Jaap J. M. Smit,§  
Alfred H. Schinkel,§  
Robbert G. E. Notenboom,‡  
Marius A. van den Bergh Weerman,\*  
Ronald P. Verkruijsen,\* Albert K. Groen,†  
Ronald P. J. Oude Elferink,†  
Martin A. van der Valk,§ Piet Borst,§ and  
G. Johan A. Offerhaus\*

From the Department of Pathology,\* Division of Gastroenterology and Hepatology,† Department of Anatomy and Embryology,‡ Academic Medical Center, Amsterdam, The Netherlands, and Division of Molecular Biology,§ The Netherlands Cancer Institute, Amsterdam, The Netherlands

**The mouse *mdr2* gene (and its human homologue MDR3, also called MDR2) encodes a P-glycoprotein that is present in high concentration in the bile canalicular membrane of hepatocytes. The 129/OlaHsd mice with a homozygous disruption of the *mdr2* gene (-/- mice) lack this P-glycoprotein in the canalicular membrane. These mice are unable to secrete phospholipids into bile, showing an essential role for the *mdr2* P-glycoprotein in the transport of phosphatidylcholine across the canalicular membrane. The complete absence of phospholipids from bile leads to a hepatic disease, which becomes manifest shortly after birth and shows progression to an end stage in the course of 3 months. The liver pathology is that of a nonsuppurative inflamma-**

**tory cholangitis with portal inflammation and ductular proliferation, consistent with toxic injury of the biliary system from bile salts unaccompanied by phospholipids. Thus, the *mdr2* (-/-) mice can serve as an animal model for studying mechanisms and potential interventions in nonsuppurative inflammatory cholangitis (in a generic sense) in human disease, be it congenital or acquired. When the mice are 4 to 6 months of age, preneoplastic lesions develop in the liver, progressing to metastatic liver cancer in the terminal phase. The *mdr2* (-/-) mice therefore also provide a tumor progression model of value for the study of hepatic carcinogenesis. Interestingly, also in this regard, the model mimicks human disease, because chronic inflammation of the biliary system in humans may similarly carry increased cancer risk. (Am J Pathol 1994, 145:1237-1245)**

MDR genes belong to a small family of closely related genes, with two members in humans<sup>1-3</sup> and three members in rodents,<sup>4-7</sup> that encode for cell membrane proteins known as P-glycoproteins (P-gps). The human *MDR1* gene<sup>2,3</sup> and the mouse *mdr1* (or *mdr1b*) and *mdr3* (or *mdr1a*) genes<sup>4,6</sup> encode P-gps that mediate the increased efflux of intracellular hy-

Supported in part by grants NKI 88-6 and 92-41 of the Dutch Cancer Society to PB.

Accepted for publication August 3, 1994.

Address reprint requests to Dr. G. J. A. Offerhaus, Department of Pathology (H2), Academic Medical Center, Meibergdreef 9, 1105 AZ Amsterdam, The Netherlands.

drophobic drugs observed in multidrug resistance (MDR).<sup>9</sup> The human *MDR3* (also called *MDR2*)<sup>1</sup> gene product and its mouse homologue the *mdr2* P-gp, however, do not confer MDR to cells and until recently their transport function was poorly understood.

Its typical distribution pattern in adult liver, with an exclusive expression at the canalicular membrane of hepatocytes,<sup>9-11</sup> suggested a role for the *mdr2* P-gp in biliary excretion. Proof for such a role was recently obtained when homozygous mice, in which the *mdr2* gene had been disrupted, were generated:<sup>12</sup> phospholipid excretion in bile was undetectable in the homozygous (*-/-*) *mdr2* mice and reduced to 60% of normal in the heterozygous (*+/-*) *mdr2* mice. Other abnormalities in the bile included a decrease of the biliary glutathione (down to 14% of controls) and cholesterol secretion (down to 7%) in the *mdr2* (*-/-*) mice, whereas in the *mdr2* heterozygotes these values were comparable to the wild-type animals. The bile acid and conjugated bilirubin output in the *mdr2* (*-/-*) mice was not different from the *mdr2* (*+/-*) and (*+/+*) mice, but the bile flow in *mdr2* (*-/-*) mice was twice that of the heterozygous *mdr2* and normal wild-type mice, presumably due to ductular proliferation (see below). In the *mdr2* (*-/-*) mice, serum bilirubin was variably (3- to 20-fold) elevated, approximately half of it being conjugated. This can be attributed to leakage from damaged hepatocytes or bile canaliculi. Liver function tests were also moderately (3- to 6-fold) elevated, consistent with damage of the liver parenchyma. In the *mdr2* (*+/-*) mice, serology was comparable to the wild-type mice and within normal limits. All available results indicate that the primary defect in the *mdr2* (*-/-*) mice is their inability to secrete phospholipids into bile.

Apparently, the *mdr2* P-gp is essential for this process and this protein may act as a phospholipid translocator or flippase,<sup>13</sup> although a more indirect effect of the protein on phospholipid transport is not excluded.<sup>12</sup> The secretion of hydrophobic bile salts in the absence of phospholipid results in damage of membranes<sup>14,15</sup> and liver disease.<sup>12</sup> This article gives a detailed description of the accompanying liver pathology and considers potential applications of the *mdr2* (*-/-*) mouse as an animal model of human hepatobiliary disease.

## Materials and Methods

### Animals

The generation of homozygous *mdr2* (*-/-*) mice lacking a functional *mdr2* gene has been described in detail previously.<sup>12</sup> In this study, mice homozygous

(*-/-*) and heterozygous (*+/-*) for the disruption of the *mdr2* gene and normal wild-type (*+/+*) mice (129/OlaHsd; Harlan UK Limited, Bicester, UK) were compared. The study group was comprised of 66 mice with ages ranging from 2 days to 1.5 years. As a routine procedure, the genotype of the mice was checked by Southern blot analysis of genomic DNA isolated from individually collected tails at sacrifice. DNA isolation and Southern blot analysis were performed according to standard techniques.<sup>16,17</sup> The mice were fed a standard diet (AM-II diet; Hope Farms, The Netherlands) and water ad libitum. Animal welfare was in accordance with the institutional guidelines of the University of Amsterdam.

### Histochemistry

Tissue samples were fixed by immersion in a mixture of ethanol, acetic acid, and formalin (8:1:2, v/v).<sup>18</sup> Five-micron thick serial paraffin sections were stained according to standard histochemical procedures with hematoxylin and eosin (H&E), periodic acid Schiff (PAS), periodic acid Schiff after diastase digestion (PAS-D), Gomorri's reticulin stain, Perl's iron, and van Gieson's elastic staining. ATPase enzyme histochemistry was conducted on selected cases with large nodules in the liver using 5- $\mu$  thick cryostat sections.

### Immunohistochemistry

Immunoperoxidase staining was performed with a panel of polyclonal (Pabs) and monoclonal antibodies (MAbs) raised against different antigens (Table 1). Tissue processing and immunohistochemistry were performed according to standard procedures (for details see Table 1). Briefly, endogenous peroxidase activity was blocked by incubation of sections in 0.3% (v/v) H<sub>2</sub>O<sub>2</sub> in methanol for 20 minutes. Nonspecific binding of immunoglobulins (Igs) was blocked by preincubation with normal goat serum (Dako A/S, Copenhagen, Denmark). Before immunostaining with the antikeratin Pab, sections were predigested with 0.25% (w/v) pepsin (Sigma, St. Louis, MO) in 10 mmol/L HCl for 15 minutes at 37 C. Likewise, sections were pretreated with 10 mmol/L citrate buffer (pH 6) for 2  $\times$  5 minutes at 100 C when the anti-Ki-67 Pab was used. Antibody binding on sections was visualized using 0.1% (w/v) 3,3'-diaminobenzidine tetrahydrochloride (Sigma) dissolved in 50 mmol/L Tris-HCl (pH 7.6) containing 0.03% (v/v) H<sub>2</sub>O<sub>2</sub> as the chromogen. Color was developed for 7 minutes. In most experiments sections were counterstained with hematoxylin.

**Table 1.** Primary Pabs and MAbs Used in this Study

Antibody	Supplier	Specificity	References*
P-gps Pab REG3 Mab C219		MDR3 and <i>mdr2</i> P-gp All mouse P-gps	Smit et al <sup>11,12</sup> Georges et al <sup>19</sup>
Proliferation markers Pab Ki-67	Dako A/S, Denmark (A 047)	395- and 345-kd polypeptides of a cell proliferation- associated nuclear antigen	Key et al <sup>20</sup> Schlüter et al <sup>21</sup>
Intermediate filament proteins Pab keratin	Dako A/S, Denmark (Z 622)	Keratin subunits of 58, 56, and 52 kd and less abundantly subunits of 60, 51, and 48 kd	Steiner <sup>22</sup> Franke et al <sup>23</sup>
Serum proteins Pab $\alpha_1$ -fetoprotein	Dako A/S, Denmark (A 008)	$\alpha_1$ -Fetoprotein	Jacobsen et al <sup>24</sup>
Pab $\alpha_1$ -fetoprotein	Obtained from Dr. S.H. Yap	$\alpha_1$ -Fetoprotein	Selten et al <sup>25</sup>
Metabolic markers Pab glutamine synthase		Glutamine synthase	de Groot et al <sup>26</sup>

\* References refer to the fixation and immunohistochemical staining method applied to reveal the expression of the antigen.

Commercially available unconjugated secondary antibodies and peroxidase antiperoxidase immunocomplexes were purchased from Nordic (Nordic, Tilburg, The Netherlands). Biotinylated swine to rabbit Igs and horseradish peroxidase-conjugated streptavidin were obtained from Dako.

### Electron Microscopy

The livers of 20 *mdr2* (-/-) and of 13 control (+/+) mice were prepared for electron microscopy. They covered the same age range, ie, from 2 days to 1.5 years, as the animals studied light microscopically. Routinely, whole livers were perfused with the aid of a peristaltic pump via the portal vein with 200 mmol/L cacodylate buffer, followed after 30 seconds by 2% (w/v) paraformaldehyde in the same buffer. In a few cases, a single lobe of a liver intended for light microscopic examination was perfused by hand via the portal branch. Dissected tissue blocks were postfixed with 1% OsO<sub>4</sub> and embedded in LX-112 resin. Before uranyl and lead staining, thin sections were briefly treated with diluted tannic acid to increase the contrast of both glycogen and extracellular elements.<sup>27</sup> In a number of samples peroxisomes were identified by means of ultrastructural catalase histochemistry.<sup>28</sup>

### Light Microscopy

Various histopathological parameters (Figure 1B) were systematically assessed to evaluate the morphology of the liver pathology that develops in the *mdr2* (-/-) mice. Some of these parameters were determined by computerized image analysis using a light microscope equipped with a charge-coupled

device monochrome video camera (AIS MX5). For the data analysis a standard image processing program (TEA Image Manager, DIFA Measuring Systems, The Netherlands)<sup>29</sup> was used.

Periportal and pericentral regions of the liver lobule were compared and arbitrarily defined as concentric layers of five hepatocytes thick surrounding the terminal branches of the portal vein or the branches of the hepatic vein.

## Results and Discussion

### Nonsuppurative Inflammatory Cholangitis in the *mdr2* (-/-) Mice and Potential Human Homologues

The *mdr2* (-/-) mice are indistinguishable from the heterozygous *mdr2* (+/-) and wild-type (+/+) mice in external appearance, mortality, growth rate, and weight during the first year of age.<sup>12</sup> The fertility of the females appears to decrease at ages more than 4 months. Thus far organs other than the liver have not shown any abnormality. All tissues were examined by light microscopy at various times after birth and compared with those of heterozygous and wild-type mice. Special attention was paid to organs where *mdr2* expression is predominantly found (ie, spleen, heart, muscle, and adrenal).<sup>12</sup> Sex differences were not seen. No morphological difference between the *mdr2* (+/-) and the wild-type control mice was observed.

The liver of the *mdr2* (-/-) mice looks anatomically normal at birth. In accordance with the literature,<sup>30</sup> the bile canaliculi of all neonatal mice (-/-, +/-, and

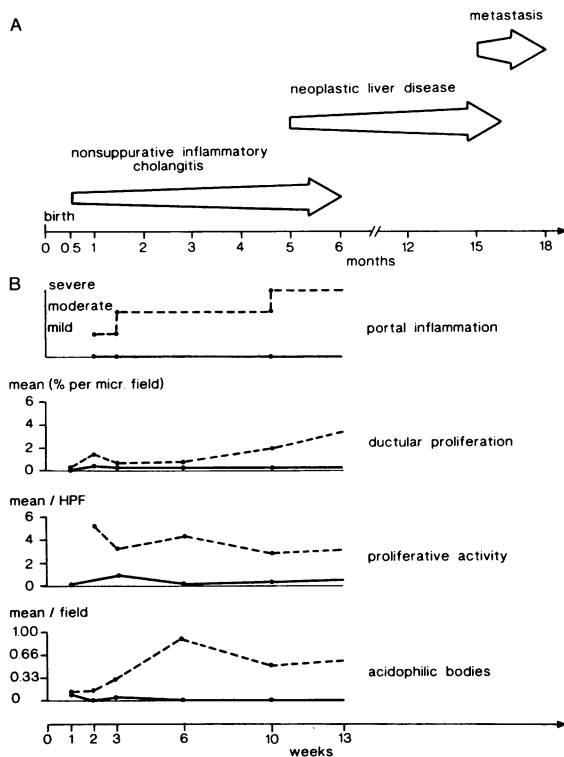


**Figure 1.** A: Schematic diagram of the nature and time sequence of the liver disease in the *mdr2* P-gp-deficient mice. B: Evolution of the main histological parameters characterizing the development of non-suppurative inflammatory cholangitis during the first 3 months. The degree of portal inflammation was graded as absent (no inflammatory cells present), light (only scattered inflammatory cells present in the mesenchyme of the portal triads), moderate (increasing inflammatory infiltrate in the portal triads associated with cholangiolitis, ie, inflammatory cells invading bile ducts, no fibrosis present), and severe (in addition to the inflammatory infiltrate, fibrosis is also present). As a measure for the extent of ductular proliferation, the size of the ductular compartment (delineated by a positive staining for the antikeratin Pab; see Figure 3B) was assessed in 10 microscopic fields at  $\times 250$  magnification using computerized image analysis. The proliferative activity was evaluated by the Ki-67 labeling index (ie, the number of positively stained nuclei for the anti-Ki-67 Pab per high-power field [HPF]), and the number of acidophilic ('Councilman') bodies were quantified in 20 randomly chosen microscopic fields at  $\times 400$  magnification. Dotted lines, *mdr2* (-/-) mice; straight lines, wild-type control (+/+) mice.

+/-) are wide and relatively smooth. In (+/+) and (+/-) mice these immature bile canaliculi develop within 2 to 3 weeks into the adult type, ie, their diameters decrease with a concomitant increase in the number of microvilli. In contrast, the immature phenotype consistently persists in the adult *mdr2* (-/-) mice and the canaliculi remain wide and smooth, whereas an excessive number of canalicular cross-sections indicates tortuosity (Figure 2). In addition, in the pericanalicular ectoplasm deposition of microf filamentous material is often present. These electron microscopic findings resemble those of cholestasis and are in itself nonspecific. Presumably, it is therefore best considered a secondary phenomenon due to the increased flow of toxic bile salts.

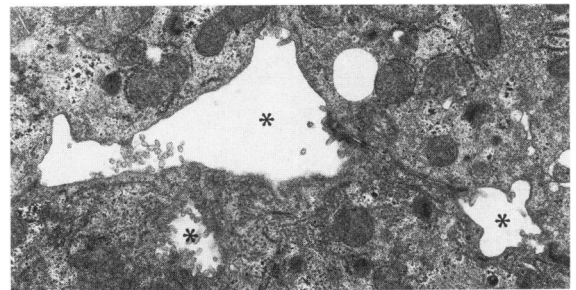


**Figure 2.** Electron microscopy of the liver of a 1-year-old *mdr2* P-gp-deficient mouse. The presence of three bile canalicular profiles (asterisks) in one field indicates an increased tortuosity of bile canaliculi. Note that the central bile canalicular profile is excessively wide and that there are only relatively few microvilli. Original magnification  $\times 9,200$ .

When these ultrastructural differences between the *mdr2* (-/-) and (+/+) mice become clear, light microscopic alterations also begin to arise, and at 2 to 3 weeks light microscopy will distinguish the *mdr2* (-/-) mice from the controls ((+/-) and (+/+)). There is ductular proliferation and portal inflammation with a mixed inflammatory infiltrate; the bile duct epithelium shows reactive changes and presence of intra-epithelial inflammatory cells (Figure 3). Throughout the lobule an increased number of acidophilic bodies and mitotic figures is seen. The proliferative activity assessed by Ki-67 labeling is increased both in the pericentral and periportal area. Because the first visible morphological changes concern the canaliculi and bile ductuli, presumably this part of the biliary tract is affected first. The light microscopic changes progress ultimately to a relatively stable end stage in the course of approximately 3 months. Although there is considerable expansion of the portal triad, biliary cirrhosis with porto-portal fibrous septa is never encountered.

Immunohistochemistry with the anti-REG3 antibody specific for *mdr2* P-gp<sup>11</sup> shows no canalicular staining in *mdr2* (-/-) mice, whereas the positive immunostaining with the C219 antibody that recognizes all three mouse P-gps, remains.<sup>11</sup> This confirms the specific loss of the canalicular *mdr2* P-gp, which leads to the complete loss of biliary phospholipid excretion.<sup>12</sup> The liver pathology is that of a nonsuppurative inflammatory cholangitis in a generic sense<sup>31</sup> and it is consistent with the postulated mechanism of toxic injury by bile salts due to a lack of biliary phospholipids.<sup>12,32</sup> That explains why morphological change does not arise until some time after birth when the bile salt secretion starts to build up.<sup>33</sup>

Nonsuppurative inflammatory duct lesions form the morphological hallmark of an important category of pathological conditions in humans, both in congenital and acquired hepatobiliary diseases.<sup>31,34</sup> Several of

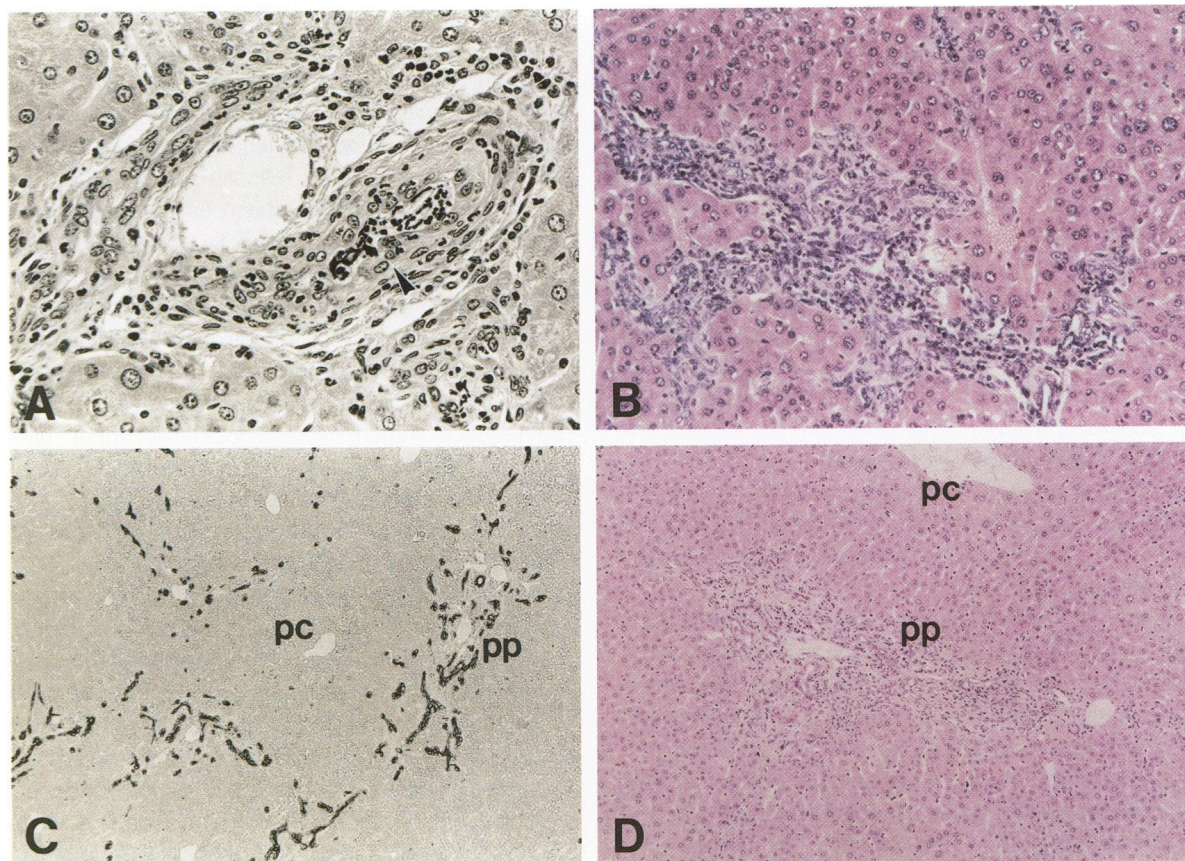


**Figure 3.** Microscopy of the liver of a 3-months-old *mdr2* P-gp-deficient mouse. **A:** Portal inflammation with inflammatory cells invading bile ducts (arrowhead) and fibrosis; H&E staining. **C:** Ductular proliferation of bile ducts extending into the parenchyma of the periportal region. Immunoperoxidase staining with the antikeratin Pab. **B, D:** Light microscopic overview of the cholangitis accompanied by prominent portal expansion due to inflammation, ductular proliferation, and fibrosis; H&E staining. pp, Periportal region; pc, pericentral region. Original magnification: A,  $\times 100$ ; B,  $\times 40$ ; C and D,  $\times 25$ .

these conditions are poorly understood and it is conceivable that a primary defect in biliary phospholipid excretion as the underlying mechanism has been overlooked.<sup>31,34-36</sup> A genetic defect, but also autoimmunity or other insults (eg, infection and drugs), might interfere with phospholipid excretion. The human MDR3 P-gp and the murine *mdr2* P-gp are very similar in all essential properties. Their amino acid sequences are more than 90% identical and their tissue distribution is the same.<sup>11</sup> The MDR3 P-gp is also abundantly present in the hepatocyte canalicular membrane,<sup>11</sup> and it is therefore very likely that it is essential for phospholipid secretion into bile in humans too. A complete absence of the MDR3 P-gp could be expected to result in rapidly progressive disease, incompatible with longstanding survival; partial defects might lead to a milder picture that could be provoked by factors that cause impairment of P-gp activity or increase of bile salt flow. Importantly, human bile salts are more hydrophobic than those of

rodents and might, therefore, lead to more aggressive disease and a more destructive or obliterative type of ductular lesions.

Of the neonatal conditions, progressive familial intrahepatic cholestasis ('Byler'-like pictures),<sup>37-39</sup> biliary atresia, and paucity of bile ducts need particular consideration.<sup>31,34,40</sup> It is at least remarkable that obliteration or destruction of the intrahepatic ducts apparently only takes place some time after birth. These ducts become patent during the first weeks of life and to our knowledge obliteration at autopsy in a stillborn has never been described.<sup>40</sup>

Acquired destructive cholangiopathies in adults, in which the pathology shows resemblance with the above category of neonatal diseases, are pictures that resemble primary biliary cirrhosis (PBC) and primary sclerosing cholangitis (PSC) but also unexplained vanishing bile duct syndromes.<sup>31,34-36,41,42</sup> These conditions too are mostly not well understood and, therefore, need consideration. In typical PBC

and PSC, we and others have not observed a decreased biliary phospholipid excretion.<sup>43</sup> Finally, interference with MDR3 P-gp function or other forms of inhibition of biliary phospholipid secretion could also underlie some of the drug reactions leading to non-suppurative cholangitis.<sup>31,44</sup> Whether loss of MDR3 function plays a role in any of the above clinical disorders characterized by cholangiocellular destruction, remains of course a theoretical and speculative concept until proven otherwise. Obviously, any other process that interferes with phospholipid synthesis or transport of phospholipid into bile could give rise to a phenocopy of MDR3 P-gp deficiency. For instance, the possibility has been raised that the hepatic phosphatidylcholine transfer protein is required for the transport of newly synthesized phosphatidylcholine to the canalicular membrane.<sup>12,45</sup> A defect in this protein might therefore also interfere with the secretion of phospholipid into bile.

Even if in humans the very same defect as in the *mdr2*(-/-) mouse is not easily traceable, the induced inflammatory cholangitis in the mouse should serve as an animal model to study potential interventions in the complex disease category of nonsuppurative cholangitis. Modulation of bile salt composition in favor of hydrophilic bile salts unable to elute phospholipid from membranes might diminish cellular injury, a therapeutic effect that might explain why some patients with PBC, PSC, and analogous diseases benefit from ursodeoxycholate administration.<sup>46-48</sup>

### Hepatocarcinogenesis in the *mdr2* (-/-) Mice

At the age of approximately 4 to 6 months the *mdr2* (-/-) mice start to develop multiple foci in the liver parenchyma, culminating in grossly visible nodular

outgrowths in the hepatectomy specimens (Figure 4, compare A with B). The irregularly enlarged livers show multiple tumors, often with necrosis and hemorrhage. Using light microscopy, the lesions consist of sheets of atypical hepatocytes with loss of the pre-existing architecture and reticulin pattern. There is strong cytonuclear polymorphism, an increased number of mitotic figures, and apoptotic bodies (Figure 5, B and C). At this stage the lesions appear relatively circumscribed and vasoinvasion has not been observed with certainty but the lesions do fulfill microscopic criteria used in chemically induced hepatocarcinogenesis to diagnose neoplastic nodules.<sup>49,50</sup> The neoplastic nature of these nodules is further supported by the observed decrease of PAS-positive glycogen in these lesions, the loss of the ATPase staining reaction in enzyme histochemistry, and the positive glutamine synthase immunostaining (Figure 5A),<sup>50,51</sup> in one case subcutaneous transplantation of preneoplastic liver tissue resulted in a tumorous outgrowth.

The nodules show a highly variable ultrastructural picture. Some are made up of small cells without peroxisomes but others consist of cells that can be recognized as hepatocytes with numerous peroxisomes, as verified by catalase histochemistry. Also in the pre-existing liver cells of older *mdr2* (-/-) mice, the number of peroxisomes is often increased. This is of interest, because it has been postulated that proliferation of peroxisomes serves as an endogenous initiator of neoplastic transformation in the liver through the production of oxygen radicals.<sup>52-54</sup> Whether peroxisome proliferation causes cancer or is part of the genetic reprogramming caused by cancer remains controversial, however.<sup>53</sup> Replication of DNA is not a flawless process and increased cell turnover increases the rate of somatic mutation. It is therefore possible that the hepatocarcinogenesis in the *mdr2*

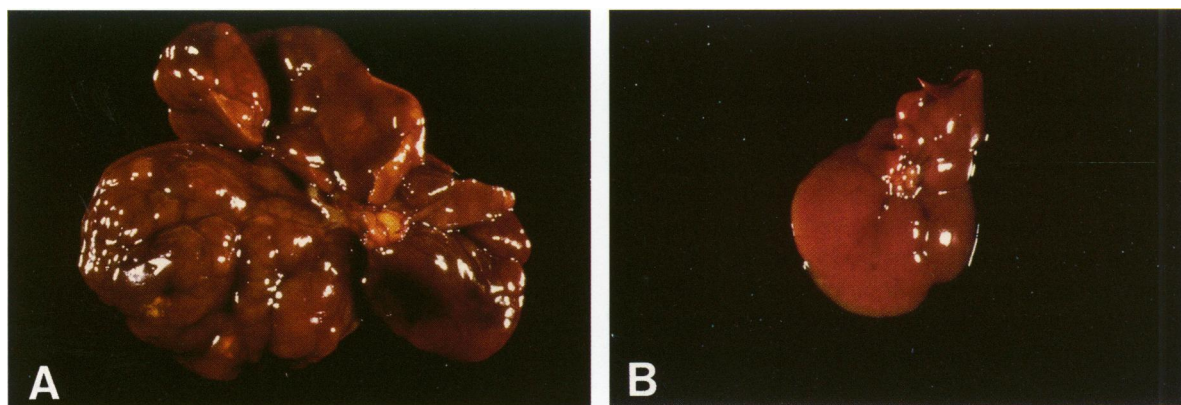
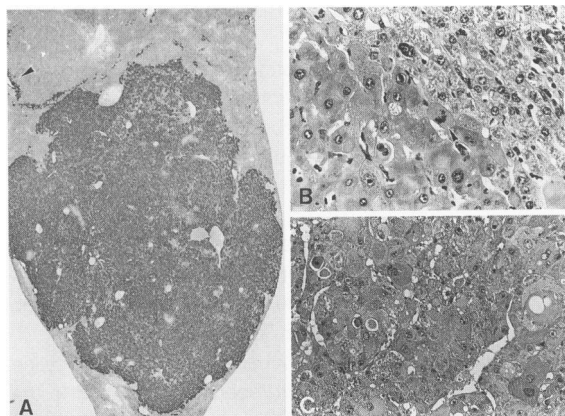
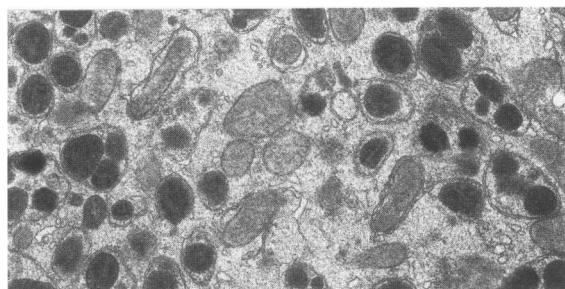


Figure 4. Macroscopy of the liver of a 6-months-old *mdr2* P-gp-deficient mouse (A) compared with a wild-type control mouse (B). Note the nodularity of the (7- to 8-fold) enlarged liver in the *mdr2* (-/-) mouse.



**Figure 5.** Microscopy of the liver of a 1-year-old *mdr2* P-gp-deficient mouse showing the features of a neoplastic nodule. **A:** Positive immunoreactivity for glutamine synthase. The original pericentral localization of glutamine synthase positivity in the preexistent liver parenchyma is indicated by the arrowhead. Immunoperoxidase staining with the antiglutamine synthase Pab. **B:** Cytonuclear polymorphism and mitotic figures (arrowhead) of hepatocytes. The lesion is relatively well demarcated; H&E staining. **C:** In addition, there is loss of the original trabecular architecture with a tendency of the liver cells to grow in sheets; H&E staining. Original magnification: **A**,  $\times 6.25$ ; **B**,  $\times 100$ ; **C**,  $\times 25$ .

( $-/-$ ) mouse only reflects the chronic liver damage and the ensuing increased rate of cell turnover. Hepatocarcinogenesis has also been seen in other conditions resulting in widespread liver necrosis in rodents, eg, choline-deficient diet.<sup>54</sup> So far, the two oldest (1.5 years of age) *mdr2* ( $-/-$ ) mice showed lung metastasis and the presence of many catalase-positive peroxisomes in these secondary tumors unequivocally confirmed their hepatocyte derivation (Figure 6). Thus, the natural history of the liver disease that accompanies the homozygous disruption of the murine *mdr2* allele apparently constitutes a tumor progression model of spontaneous hepatocarcinogenesis. Also, in this regard, a link with human disease can be seen because chronic inflammation of



**Figure 6.** Electron microscopy of lung metastasis of a 1.5-year-old *mdr2* P-gp-deficient mouse. Only a small cytoplasmic part of one cell is shown. Note that peroxisomes are abundantly present. Catalase histochemistry has been used to increase the electron density of peroxisomes. Original magnification  $\times 21,000$ .

the biliary system in humans may similarly carry cancer risk, although in that event the cholangiocellular phenotype appears as the preferred lineage.

Further studies are needed to delineate the precise nature of the neoplasms in the livers of the *mdr2* ( $-/-$ ) mice but the mouse could serve as a valuable adjunct in the current debates on liver stem cells.<sup>55-57</sup> Importantly,  $\alpha_1$ -fetoprotein positivity was not seen in the *mdr2* ( $-/-$ ) mice; at the terminal ends of the bile ductules, epithelial cells were, however, found that bordered directly on the hepatocytes, often in irregular groups without a recognizable lumen. These cells might therefore be transition duct cells.<sup>58</sup> Using recently described ultrastructural criteria,<sup>59</sup> we could not easily detect oval cells by electron microscopy. The glutamine synthase positivity that accompanies the neoplastic transformation may also point to a specific cell lineage but then from a pericentral origin.<sup>51,60</sup>

In conclusion, the *mdr2* ( $-/-$ ) mouse not only serves as an interesting model for studies of nonsuppurative inflammatory cholangitis, but further studies of the tumors that eventually arise in the livers of these mice may also contribute to a better understanding of hepatocarcinogenesis.

### *Availability and Biological Features*

The *mdr2* P-gp-deficient mouse is available for other investigators. The 129/OlaHsd strain is generally regarded as a poor breeder and the mice generate limited offspring. The fertility in the female *mdr2* ( $-/-$ ) mice even decreases after 4 months. Therefore, the 129/OlaHsd *mdr2* ( $-/-$ ) mice were intercrossed and further backcrossed to FVB/N0laHsd mice. The FVB/N *mdr2* ( $-/-$ ) mice have a phenotype identical to that of the 129/OlaHsd during the first 3 to 4 months. The long-term picture, however, is yet unknown.

### *Acknowledgments*

We thank Dr. S. H. Yap for his kind gift of the  $\alpha$ -fetoprotein antiserum to the Department of Anatomy and Embryology. We are grateful to Ms. Gina Beekelaar for help with the preparation of the manuscript, to Mr. Wilfried Meun for microphotography and macrophotography, and to Mr. Roel Ottenhoff for taking care of the animals. Drs. Fibo ten Kate, Ewald Scherer, Frank Baas, and Frits Wijburg are gratefully acknowledged for their stimulating suggestions.

## References

1. Roninson IB, Chin JE, Choi K, Gros P, Housman DE, Fojo A, Shen D-W, Gottesman MM, Pastan I: Isolation of human *mdr* DNA sequences amplified in multidrug-resistant KB carcinoma cells. *Proc Natl Acad Sci USA* 1986, 83:4538-4542
2. Ueda K, Cardarelli C, Gottesman MM, Pastan I: Expression of full-length cDNA for the human MDR1 gene confers resistance to colchicine, doxorubicin, and vinblastine. *Proc Natl Acad Sci USA* 1987, 84:3004-3008
3. Lincke CR, van der Blik A, Schuurhuis GJ, van der Velde-Koerts T, Smit JJM, Borst P: The multidrug resistance phenotype of human BRO melanoma cells transfected with a wild-type human *mdr1* cDNA. *Cancer Res* 1990, 50:1779-1785
4. Gros P, Neriah YB, Croop JM, Housman DE: Isolation and expression of a cDNA (*mdr*) that confers multidrug resistance. *Nature* 1986, 323:278
5. Gros P, Raymond M, Bell J, Housman D: Cloning and characterization of a second member of the mouse *mdr* gene family. *Mol Cell Biol* 1988, 8:2770-2778
6. Devault A, Gros P: Two members of the mouse *mdr* family confer multidrug resistance with overlapping but distinct drug specificities. *Mol Cell Biol* 1990, 10:1652-1653
7. Endicott JA, Sarangi F, Ling V: Complete cDNA sequences encoding the Chinese hamster P-glycoprotein gene family. *J DNA Seq Map* 1991, 2:89-101
8. Gerlach JH, Kartner N, Bell DR, Ling V: Multidrug-resistance. *Cancer Surv* 1986, 5:25-46
9. Cordon-Cardo C, O'Brien JP, Boccia J, Casals D, Bertino JR, Melamed MR: Expression of the multidrug resistance gene product (P-glycoprotein) in human normal and tumor tissues. *J Histochem Cytochem* 1990, 38:1227-1287
10. van der Valk P, van Kalken CK, Ketelaars H, Broxterman HJ, Scheffer G, Kuiper CM, Tsuruo T, Lankelma J, Meijer CJLM, Pinedo HM, Scheper RJ: Distribution of multi-drug resistance-associated P-glycoprotein in normal and neoplastic human tissues. *Ann Oncol* 1990, 1:56-65
11. Smit JJM, Schinkel AH, Mol CAAM, Majoor D, Mooi WJ, Jongsma APM, Lincke CR, Borst P: The tissue distribution of the human MDR3 P-glycoprotein. *Lab Invest* 1994 (in press)
12. Smit JJM, Schinkel AH, Oude Elferink RPJ, Groen AK, Wagenaar E, van Deemter L, Mol CAAM, Ottenhoff R, van der Lugt NMT, van Roon MA, van der Valk MA, Offerhaus GJA, Berns AJM, Borst P: Homozygous disruption of the murine *mdr2* P-glycoprotein gene leads to a complete absence of phospholipid from bile and to liver disease. *Cell* 1993, 75:451-462
13. Higgins CF, Gottesman M: Is the multidrug transporter a flippase? *Trends Biochem Sci* 1992, 17:18-21
14. Barnwell SB, Tuchweber B, Yousef IM: Biliary lipid secretion in the rat during infusion of increasing doses of unconjugated bile acids. *Biochim Biophys Acta* 1987, 922:221-233
15. Yousef IM, Barnwell S, Gattton F, Tuchweber A, Roy CC: Liver cell membrane solubilization may control maximum secretory rate of cholic acid in the rat. *Am J Physiol* 1987, 252:G84-G91
16. Sambrook J, Fritsch EF, Maniatis T: *Molecular Cloning: A Laboratory Manual*, ed 2. Cold Spring Harbor, New York, Cold Spring Harbor Laboratory Press, 1989
17. Laird PW, Zijderveld A, Linders K, Rudnicki MA, Jaenish R, Berns A: Simplified mammalian DNA isolation procedure. *Nucleic Acids Res* 1991, 19:4293
18. Harrison, PTC: An ethanol-acetic acid-formol saline fixative for routine use with special application to the fixation of non-perfused rat lung. *Lab Animal* 1984, 18:325-331
19. Georges E, Bradley G, Garipey J, Ling V: Detection of P-glycoprotein isoforms by gene specific monoclonal antibodies. *Proc Natl Acad Sci USA* 1990, 87:152-156
20. Key G, Petersen JL, Becker MH, Duchrow M, Schlüter C, Askaa J, Gerdes J: New antiserum against Ki-67 antigen suitable for double immunostaining of paraffin wax sections. *J Clin Pathol* 1993, 46:1080-1084
21. Schlüter C, Duchrow M, Wohlenberg C, Becker MHG, Key G, Flad H-D, Gerdes J: The cell proliferation-associated antigen of antibody Ki-67: a very large, ubiquitous nuclear protein with numerous repeated elements, representing a new kind of cell cycle-maintaining proteins. *J Cell Biol* 1993, 123:513-522
22. Steiner PM: The extraction and characterization of bovine epidermal  $\alpha$ -keratin. *Biochem J* 1975, 149:39-48
23. Franke WW, Weber K, Osborn M, Schmid E, Freudenstein C: Decoration of tonofilament-like arrays in various cells of epithelial character. *Exp Cell Res* 1978, 116:429-445
24. Jacobsen GK, Jacobsen M, Clausen PP: Distribution of tumor-associated antigens in the various histologic components of germ cell tumors of the testis. *Am J Surg Pathol* 1981, 5:257-266
25. Selden GCM, Selden-Versteegen AME, Yap SH: Expression of alpha-fetoprotein and albumin genes in rat hepatoma cell line SY/1/80: evidence for the need of species specific serum factors. *Biochem Biophys Res Commun* 1981, 103:278-284
26. de Groot CJ, ten Voorde GHJ, van Andel RE, te Kortschot A, Gaasbeek, Janzen JW, Wilson RH, Moorman AFM, Charles R, Lamers WH: Reciprocal regulation of glutamine synthetase and carbamoylphosphate synthetase levels in rat liver. *Biochim Biophys Acta* 1987, 908:231-240
27. Dingemans KP, van den Bergh Weerman MA: Rapid contrasting of extracellular elements in thin sections. *Ultrastruct Pathol* 1990, 14:519-527
28. Roels F, Cornelis A: Heterogeneity of catalase staining in human hepatocellular peroxisomes. *J Histochem Cytochem* 1989, 37:331-337
29. Groen FCA, Ekkers RJ, de Vries R: Image processing with personal computers. *Signal Process* 1988, 15:279-291



30. de Wolf-Peeters C, de Vos R, Desmet V, Branchi L, Rohr HP: Electron microscopy and morphometry of canalicular differentiation in fetal and neonatal rat liver. *Exp Mol Pathol* 1972, 21:339-350
31. Ludwig J, Czaja AJ, Dickson ER, LaRusso NF, Wiesner RH: Manifestations of nonsuppurative cholangitis in chronic hepatobiliary diseases: morphologic spectrum, clinical correlations and terminology. *Liver* 1984, 4:105-116
32. Guldutuna S, Zimmer G, Imhof M, Bhatti S, You T, Leuschner U: Molecular aspects of membrane stabilization by ursodeoxycholate. *Gastroenterology* 1993, 104:1736-1744
33. Suchy FJ, Bucuvalas JC, Goodrich AL, Moyer MS, Blitzer BL: Taurocholate transport and Na<sup>+</sup>/K<sup>+</sup>-ATPase activity in fetal liver and neonatal rat liver plasma membrane vesicles. *Am J Physiol* 1986, 251:G665-G673
34. Balistreri WF: Mechanisms and management of pediatric hepatobiliary disease. *J Pediatr Gastr Nutr* 1990, 10:138-147
35. Taylor SL, Dean PJ, Riely CA: Primary autoimmune cholangitis: an alternative to antimitochondrial antibody-negative primary biliary cirrhosis. *Am J Surg Pathol* 1994, 18:91-99
36. Micheletti P, Wanless IR, Katz A, Scheuer PJ, Yeaman SJ, Bassendine FM: Antimitochondrial antibody negative primary biliary cirrhosis: a distinct syndrome of autoimmune cholangitis. *Gut* 1994, 35:260-265
37. Clayton RJ, Iber FL, Ruebner BH, McKusick VA: Byler disease: fatal familial intrahepatic cholestasis in an Amish kindred. *Am J Dis Child* 1969, 117:112-124
38. Nielsen IM, Ornvold K, Brock Jacobsen B, Ranek L: Fatal familial cholestatic syndrome in Greenland Eskimo children. *Acta Paediatr Scand* 1986, 75:1010-1016
39. Winkhofer-Roob BM, Shmerling DH, Soler R, Briner J: Progressive idiopathic cholestasis presenting with profuse watery diarrhoea and recurrent infections (Byler's disease). *Acta Paediatr* 1992, 81:637-640
40. Gautier M, Eliot N: Extrahepatic biliary atresia. Morphological study of 98 biliary remnants. *Arch Pathol Lab Med* 1981, 105:397-402
41. Zafrani ES, Metreau J-M, Douvin C, Larrey D, Massari R, Reynes M: Idiopathic biliary ductopenia in adults: a report of five cases. *Gastroenterology* 1990, 99:1823-1828
42. Faa G, van Eyken P, Demelia L, Vallebona E, Costa V, Desmet VJ: Idiopathic adulthood ductopenia presenting with chronic recurrent cholestasis. *J Hepatol* 1991, 12:14-20
43. Roda E, Mazzella G, Bazzoli F, Villanova N, Minutello A, Simoni P, Ronchi M, Poggi C, Festi D, Aldini R, Roda A: Effect of ursodeoxycholic acid administration on biliary lipid secretion in primary biliary cirrhosis. *Digest Dis Sci* 1989, 34 (Suppl):52S-58S
44. Stricker BHC: Drug Induced Hepatic Injury: Drug Induced Disorders. Edited by Dukes MNG. Amsterdam, Elsevier, 1992, pp 71-524
45. Cohen DE, Leonard MR, Carey MC: Submicellar bile salt concentrations stimulate biliary phosphatidylcholine (PC) transfer from model endoplasmic reticulum to canalicular membranes via hepatic PC-transfer protein. *Hepatology* 1992, 16:90A (abstract 181)
46. Katagiri K, Nakai T, Hoshino M: Tauro- $\beta$ -muricholate preserves cholestasis and prevents taurocholate induced cholestasis in colchicine-treated rat liver. *Gastroenterology* 1992, 102:1660-1667
47. Poo JL, Feldman G, Erlinger S, Brailon A, Gaudin C, Dumont M, Lebrec D: Ursodeoxycholic acid limits liver histologic alterations and portal hypertension induced by bile duct ligation in the rat. *Gastroenterology* 1992, 102:1752-1759
48. Kaplan MM: New strategies needed for treatment of primary biliary cirrhosis? *Gastroenterology* 1993, 104:651-653
49. Vesselinovitch SD: Invasiveness, metastasis and transplantability of mouse liver nodules: mouse liver tumors. *Arch Toxicol* 1987, 10 (Suppl):29-42
50. Scherer E: Relationship among histochemically distinguishable early lesions in multistep-multistage hepatocarcinogenesis: mouse liver tumors. *Arch Toxicol* 1987, 10 (Suppl):81-94
51. Gebhardt R, Tanaka T, Williams GM: Glutamine synthetase heterogeneous expression as a marker for the cellular lineage of preneoplastic and neoplastic liver-populations. *Carcinogenesis* 1989, 10:1917-1923
52. Reddy JK, Lalwani ND, Qureshi SA, Reddy MK, Moehle CM: Introduction of hepatic peroxisome proliferation in nonrodent species including primates. *Am J Pathol* 1984, 114:171-183
53. Rao MS, Reddy JK: An overview of peroxisome proliferator-induced hepatocarcinogenesis. *Environ Health Persp* 1991, 93:205-209
54. Ghoshal AK, Farber E: Biology of disease: choline deficiency, lipotrope deficiency and the development of liver disease including liver cancer: a new perspective. *Lab Invest* 1993, 68:255-260
55. Fausto N: Oval cells and liver carcinogenesis: an analysis of cell lineages in hepatic tumors using oncogene transfection techniques. *Prog Clin Biol Res* 1990, 331:325-334
56. Gerber MA, Thung SN: Liver stem cells and development. *Lab Invest* 1993, 68:253-254
57. Sell S: Liver stem cells. *Modern Pathol* 1994, 7:105-112
58. Novikoff PM, Ikeda T, Hixson DC, Yam A: Characterizations of and interactions between bile ductule cells and hepatocytes in early stages of rat hepatocarcinogenesis induced by ethionine. *Am J Pathol* 1991, 139:1351-1368
59. de Vos R, Desmet V: Ultrastructural characteristics of novel epithelial cell types identified in human pathologic liver specimens with chronic ductular reaction. *Am J Pathol* 1992, 140:1441-1450
60. Gebhardt R: Heterogeneous intrahepatic distribution of glutamine synthetase. *Acta Histochem* 1990, 40 (Suppl):23-28